Fifty-six years of Surface Solar Radiation and Sunshine Duration ~~at the Surface in~~ over São Paulo, Brazil: 1961 - 2016

Marcia Akemi Yamasoe[1], Nilton Manuel Évora do Rosário[2], Samantha Novaes Santos Martins Almeida[3], Martin Wild[4]

[1] Departamento de Ciências Atmosféricas, Instituto de Astronomia, Geofísica e Ciências Atmosféricas, Universidade de São Paulo, São Paulo, Brazil

[2] Departamento de Ciências Ambientais, Universidade Federal de São Paulo, Diadema, São Paulo, Brazil

[3] Seção de Serviços Meteorológicos do Instituto de Astronomia, Geofísica e Ciências Atmosféricas, Universidade de São Paulo, São Paulo, Brazil

[4] Institute for Atmospheric and Climate Science, ETH Zurich, Switzerland

Correspondence to: M. A. Yamasoe (marcia.yamasoe@iag.usp.br)

Abstract

Fifty-six years (1961 – 2016) of daily surface downward solar irradiation, sunshine duration, diurnal temperature range and the fraction of the sky covered by clouds in the city of São Paulo, Brazil, were analyzed. The main purpose was to contribute to the characterization and understanding of the dimming and brightening effects on solar global radiation in this part of South America. As observed in most of the previous studies worldwide, in this study, during the period between 1961 up to the early 1980's, more specifically up to 1983, a negative trend of about -0.40 kJm^{-2} per decade, with a significance level of $p = 0.101$ in surface solar irradiation was detected in São Paulo, characterizing the occurrence of a dimming effect. A similar behavior, a negative trend, was also observed for sunshine duration and the diurnal temperature range, the three variables in opposition to the trend in the sky cover fraction of 2.9 % per decade ($p = 0.013$). However, a brightening effect, as observed in western industrialized countries in more recent years, was not observed. Instead, for surface downward irradiation, the negative trend persisted, with a trend of -0.39 kJm^{-2} per decade ($p = 0.003$) and ~~still~~ in consonance to the cloud cover fraction increasing trend of 0.8 % per decade ($p = 0.075$). The trends for sunshine duration and the diurnal temperature range, by contrast, changed signal. Some possible causes for the discrepancy were discussed, such as the frequency of fog occurrence, urban heat island effects, horizontal visibility (as a proxy for aerosol loading variability)~~aerosol changes~~ and greenhouse gas concentration increase. Future studies on aerosol effect are ~~encouraged~~planned, particularly with higher temporal resolution as well as modeling studies, to better analyze the contribution of each possible causes.

Formatado: Não Realce

Formatado: Não Realce

Formatado: Não Realce

Formatado: Não Realce

Formatado: Não Realce

1 Introduction

Ultimately, the downward solar radiation at the surface is the main source of energy that drives Earth's biological, chemical and physical processes (Wild et al., 2013, Kren et al., 2017), from local to global scales. Therefore, the assessment of the variability of the downward solar radiation at the surface is a key step in the efforts to understand Earth's climate system variability. Before reaching the surface, solar radiation can be attenuated mainly by aerosols and clouds, through scattering and absorption processes, and to a lesser extent, through Rayleigh scattering by atmospheric gases, absorption by ozone and water vapor, for example. In this context, during the last half-century, long term changes in the amount of surface solar radiation~~ (SSR)~~ have been investigated worldwide (Dutton et al., 1991, Stanhill and Cohen 2001, Wild et al. 2005, Shi et al., 2008, Wild, 2009, 2012, Ohvril, et al., 2009). At least two trends have been well established and documented over wide regions of the world, a decline in surface solar radiation between 1950s and 1980s, named "Global Dimming" and an increase, from 1980s to 2000s, termed "Brightening" (Stanhill and Cohen, 2001; Wild, 2009, 2012).

The global dimming definition, according to Stanhill and Cohen (2001), refers to a widespread and significant reduction in global irradiance, that is the flux of solar radiation reaching the earth's surface ~~both in~~comprising the direct solar beam and ~~in ~~the diffuse radiation scattered by the sky and clouds. However, among these studies, while the dimming phase has been a consensus for all locations analyzed, the brightening phase was not (Zerefos et al., 2009, Wild, 2012). Over India, for example, the dimming phase seems to last throughout the 2000s (Kumari and Goswami, 2010). The continuous dimming in India and the renewed dimming in China from 2000s, opposing to a persistent brightening over Europe and the United States, have been linked to trends in atmospheric anthropogenic aerosol loadings (Wild, 2012). By contrast, other studies suggested that changes in cloud cover rather than anthropogenic aerosol emissions played a major role in determining solar dimming and brightening during the last half century (Stanhill et al., 2014). Therefore, the drivers of dimming and brightening are a matter of ongoing research and debate (Manara et al., 2016, Kazadzis et al., 2018, Manara et al., 2019, Yang et al. 2019). The role of these trends in the masking of temperature increase due to ~~the~~ increasing greenhouse gases (GHG) concentration has been discussed (Wild et al., 2007). Furthermore, a comprehensive assessment of the spatial scale of both dimming and brightening is critical for a conclusive analysis of the likely drivers and implications for the current global climate variability. Large portions of the globe are still lacking any evaluation on this matter, such as Africa (Wild, 2009), which is a challenge for the spatial characterization of both dimming and brightening trends.

Among the rare studies focusing on the South American subcontinent, Raichijk (2012) discussed the trends over South America, analyzing sunshine duration (SD) data from 1961 to 2004. The author divided South America in five climatic regions. In three of them, also the one where the city of São Paulo is located, statistically significant negative trends were observed on an annual basis, from 1961 up to 1990. From 1991 to 2004 a positive trend was observed in four of the five regions with a significance level higher than 90%.

The alternative use of SD is mainly due to the lack of a consistent long-term network for the monitoring of ~~SSR~~ surface solar radiation across the continent, therefore alternative proxies have to be found in order to provide an estimate of ~~SSR~~ surface solar radiation long term trends. Another variable commonly used to investigate ~~SSR~~ surface solar radiation trends is the diurnal temperature range (DTR), the difference between daily maximum (T_{max}) and minimum (T_{min}) air temperature measured near the surface (Bristow and Campbell, 1984, Wild et al. 2007, Makowski et al. 2008).

The present study takes advantage of fifty-six years of a unique high quality concurrent records of surface solar irradiation (SSR), sunshine duration (SD), diurnal temperature range (DTR) and ~~sky~~ cloud cover fraction (~~S~~CCF), i.e., the fraction of the sky covered by clouds, from 1961 to 2016, in the city of São Paulo, Brazil, to provide a perspective on dimming and brightening trends with an extended database.

T~~hus, we propose to answer t~~wo questions are addressed in this study: 1) How was the decadal~~-~~ variability of SSR over the 56 years of data?; 2) Can SD and DTR be adopted as proxies to infer SSR variability in São Paulo? To answer to these questions, we organize the manuscript as follows: in ~~part~~ section 2 we present the data and methods of analysis; section 3 is divided in 3 parts. In the first part of that section, we discuss the annual trends in SSR, SD and DTR; in the second, we focus the analysis on horizontal visibility and the number of foggy days; and ~~cloud-free days;~~ in the third part of section 3 we discuss the trends in the maximum and minimum air temperatures near the surface. Section 4 summarizes the main conclusions and discusses possible future work on the subject.

2 Observational Data and Methods

The long term measurements used in this study were collected at the meteorological station operated by the Instituto de Astronomia, Geofísica e Ciências Atmosféricas from the Universidade de São Paulo (IAG/USP), located at latitude 23.65º S and longitude 46.62º W, 799 m above sea level. Figure 1 shows the

Formatado: Não Realce

Formatado: Não Realce

geographical location of the meteorological station. The site is surrounded by a vegetated area due to its location inside a park.

Figure 1 – São Paulo state and a zooming in view of São Paulo Metropolitan Area and the location of the meteorological station of Instituto de Astronomia, Geofísica e Ciências Atmosféricas from Universidade de São Paulo (EM-IAG). Adapted from © Google Earth (US Dept. of State Geographer – Data SIO, NOAA, U. S. Navy, NGA, GEBCO - Image Landsat/Copernicus).

The downward solar irradiation has been measured since 1961 using an Actinograph Robitzsch-Fuess~~Fuess~~ model 58d, with 5% instrumental uncertainty (Plana-Fattori and Ceballos, 1988). Long-term variation of the sensor calibration of -1.5 % per decade was taken into account. This trend was estimated by comparing one year of data collected in parallel and at the same site with a brand new Actinograph Robitzsch-Fuess model 58dc, in 2014 and agrees with previous estimation performed by Plana-Fattori and Ceballos (1988) (See supplementary information for details of the comparison). Sunshine duration data was collected with a Campbell-Stokes sunshine recorder (Horseman et al., 2008) from 1933 to the present, while daily maximum and minimum air temperatures started to be monitored in 1935. Daily maximum and minimum temperatures were used to estimate the diurnal temperature range as it is simply the difference between the maximum and minimum daily temperatures. Diurnal

Formatado: Fonte: Não Itálico

Formatado: Fonte: Não Negrito

Formatado: Não Realce

Formatado: Não Realce

~~sky~~ cloud cover fraction was determined from visual inspection made every hour from 7:00 AM to 6:00 PM (local time) (Yamasoe et al. 2017).

Annual mean values of downward solar irradiation data at the surface were used to characterize dimming and brightening trends while sunshine duration and diurnal temperature range measurements at the same site were used to provide independent information.

In order to detect possible temporal changes, avoiding autocorrelation in the data, the modified Mann-Kendall trend test proposed by Hamed and Rao (1998) was applied to the variables, while the regression coefficient was estimated based on Sen (1968). A statistically significant trend at the 95% confidence level was detected if the absolute value of Z was above 1.96.

According to the meteorological station records, completely cloud free days are extremely rare in São Paulo, being more common from June to the beginning of September, corresponding to the southern hemisphere winter time, when dry conditions prevail in the region (Yamasoe et al., 2017). The number of days without clouds per year, from sunrise to sunset, varied from 1 to 23. This extremely low number of clear sky days restricted the analysis in such conditions, mainly at aiming to evaluate the exclusive role of aerosol variability in the long-term trends.

Formatado: Não Realce

To complement the analysis and help interpreting the findings, we included data about the occurrence of fog and horizontal visibility. The first information was analysed in terms of the number of foggy days (NFD). If fog was observed on a given day, the day received the number 1, otherwise, the number is 0. Horizontal visibility, or simply visibility, is recorded every hour, from 7:00 A.M. till midnight, at the meteorological station. Visibility can be affected by haze and fog conditions but is less sensitive to cloud variability. Thus, all-sky visibility data was used as a proxy for aerosol loading

Formatado: Não Realce

(Zhang et al., 2020). However, to avoid the effect of fog on the horizontal visibility, we limited the data from 10:00 AM to 03:00 PM, as, at the location, fog is usually observed either early in the morning or late in the afternoon, when low temperature and high humidity scenarios are more likely to occur in São Paulo. Therefore, the reduction in visibility from 10:00 AM to 03:00 PM is expected to be related to the atmospheric turbidity. The impact of aerosol in SSR is higher from August to October, when advection of smoke plume from long range transport can reach São Paulo, summing up to the typical increase in the local pollution associated with the dominance of low dispersion scenarios during this time of the year (Yamasoe et al., 2017). This is also when low temperatures and stable atmospheric conditions favour fog formation. Thus, the analysis of both variables is limited to the months of July to October.

To verify if the effect of visibility on SSR and SD could be detected, data measured on clear sky days were analysed normalizing SSR by the expected irradiation at the top of the atmosphere (TSR), determining the solar transmittance and minimizing the seasonal variability. Sunshine duration (SD or n) was normalized to the day-length (N). Top of the atmosphere irradiation and the day-length were estimated using formulas proposed by Paltridge and Platt (1976), which also include the variation of Sun-Earth distance.

Also, the impact of aerosol in SSR is higher from August to October, when advection of smoke plume from long range transport can reach São Paulo, summing up to the local pollution. Thus, in order to analyze how clear sky conditions varied during the last 56 years, we restricted the data to the months of July to October, to minimize the effect of any possible seasonal drift in the aerosol characteristics throughout the years. Following Manara et al. (2016), days with SCF of up to 0.1 were allowed, in

Formatado: Não Realce

Formatado: Não Realce

Formatado: Não Realce

Formatado: Não Realce

order to increase the number of clear days per year. Thus, only years with 9 or more days, in the specified months, were included in the study.

For the analysis, atmospheric transmittance was estimated dividing the measured daily surface irradiation (SSR) by the expected irradiation at the top of the atmosphere (TSR). Daily measured sunshine duration (SD or n) was also normalized to the day-length (N). Top of the atmosphere irradiation and day length were estimated using formulas proposed by Paltridge and Platt (1976). Observers at the meteorological station also take note on the occurrence of fog every day. If fog was observed, the day received the number 1, otherwise, the number is 0. For each clear sky day, information on fog observation was verified. The fraction of cloud free days with foggy conditions for each year was then estimated for the months of July to October, to verify any possible influence on SSR and SD. Moreover, since horizontal visibility information is also registered at the same time as the sky cover fraction, we included this information in this analysis as well. Table 1 presents the registered code for horizontal visibility and the corresponding distance range. Horizontal visibility can also be affected by haze and fog conditions but is less sensitive to cloud variability.

Formatado: Espaço Antes: 6 pt

Table 1 – Adopted codes for visibility records at the meteorological station and corresponding distance ranges.

Code	Distance (meter)
0	Less than 50
1	50 to 200
2	200 to 500
3	500 to 1000
4	1000 to 2000
5	2000 to 4000
6	4000 to 10000

7	10000 to 20000
8	20000 to 50000
9	> 50000

To complement the analysis, aerosol columnar loading information from satellite products such as the Absorbing Aerosol Index (AAI) from multi-sensor retrievals (TOMS, GOME-1, SCIAMACHY, OMI, GOME-2A and GOME-2B) (Herman et al., 1997, Torres et al., 1998, Graaf et al., 2005, Tilstra et al., 2014) and aerosol optical depth (AOD) from MODIS (Moderate Resolution Imaging Spectroradiometer) onboard Terra and Aqua satellites (Kaufman et al., 1997) were included. Shortly, the Absorbing Aerosol Index indicates the presence of aerosol particles in the atmosphere with high absorption efficiency in the ultraviolet spectrum. The product analyzed is the annual mean value with a spatial resolution of 1º by 1º in a box from 47º W to 46º W and 24º S to 23º S which includes São Paulo Metropolitan Area, for the months of July to October, from 1979 up to 2016 (http://www.temis.nl/airpollution/absaai/). The AOD product is a combination of the Dark Target (Kaufman et al., 1997, Remer et al., 2005) and the Deep Blue (Hsu et al., 2014) retrieval algorithms also degraded to the spatial resolution of 1º by 1º, averaged annually from 2000 (for Terra) and 2002 (for Aqua) to 2016, also considering only the dry season months obtained from the NASA Giovanni dataset site (https://giovanni.gsfc.nasa.gov/giovanni/).

3 Results

3.1 SSR, SD, DTR and SCF annual mean variability and trends

Figure 2 illustrates the time series of the annual mean values for SSR, SD, DTR and SCF, showing that all the analyzed variables exhibited a large variability from year to year. SSR, SD and DTR presented a decaying trend up to the beginning of the 1980's, in opposition, therefore consistent, to the SCF trend. According to Rosas et al. (2019), who analyzed the same cloud fraction database from the meteorological station, focusing on the climatology for different cloud types and base heights, all cloud types, except for middle level clouds, presented a positive trend, which is confirmed by this study. A statistically significant trend, at the 95% level, was observed for stratiform cloud fraction of 4.8 % per decade and for cirrus of 1.4 % per decade, from 1958 to 19868.

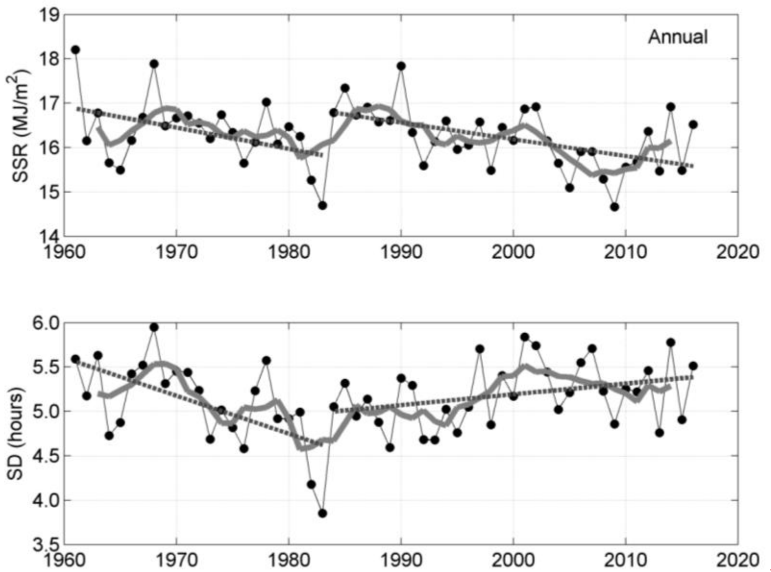

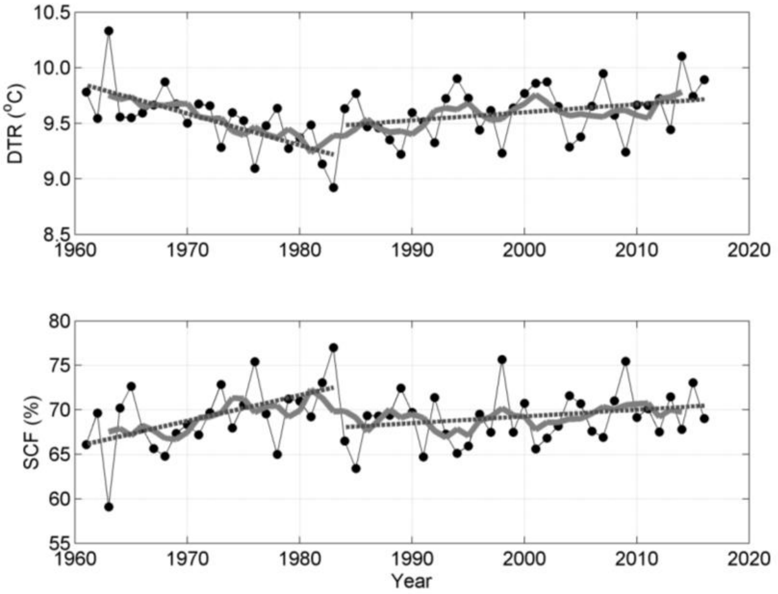
DTR (°C)
10.5
10.0
9.5
9.0
8.5
1960
1970
1980
1990
2000
2010
2020
SCF (%)
80
75
70
65
60
55
1960
1970
1980
1990
2000
2010
2020
Year

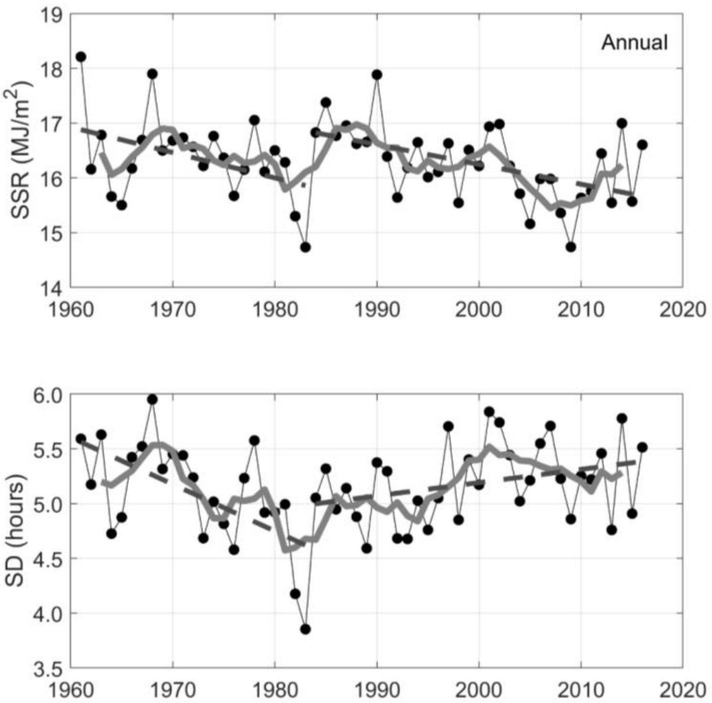

Annual
SSR (MJ/m^2)
SD (hours)
19
18
17
16
15
14
6.0
5.5
5.0
4.5
4.0
3.5
1960
1970
1980
1990
2000
2010
2020

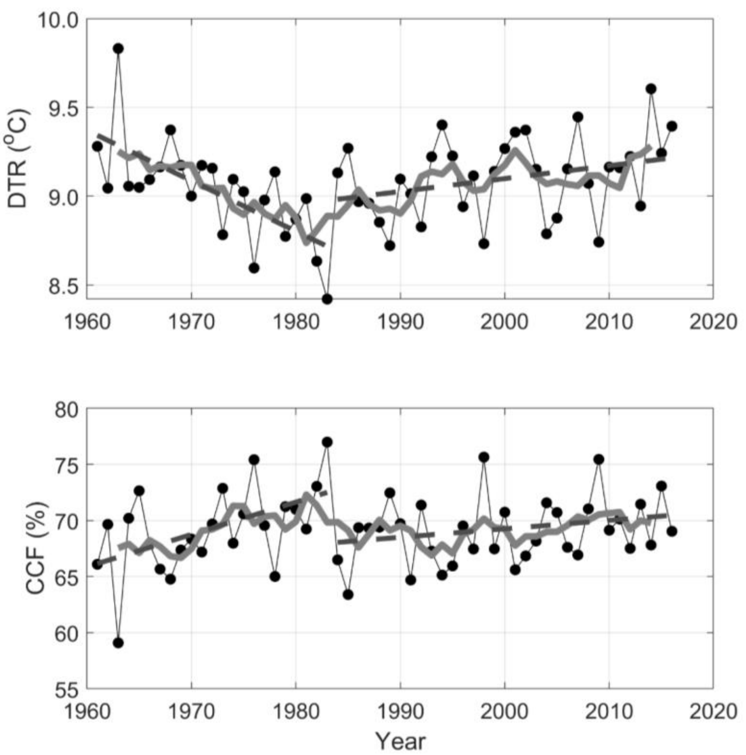

Figure 2 – Annual mean variability of surface solar irradiation (SSR), sunshine duration (SD), diurnal temperature range (DTR) and ~~sky~~ cloud cover fraction (~~S~~CCF). Gray curves represent 5 years moving averages and dotted lines are the result of trend analysis from 1961 to 1983 and from 1984 to 2016.

Returning to Figure 2, the gray curve represents the 5 years moving average, while the dotted line indicates the result of the modified Mann-Kendall trend analysis, discussed ahead. The year of 1983 was the one presenting the lowest annual mean value for SSR, SD and DTR, clearly as a response to the peak of ~~SCF~~ CCF observed in that year, which is worth to mention, was characterized by a strong El Niño event. According to the Earth System Research Laboratory from the National Oceanic and Atmospheric Administration (ESRL/NOAA), it is listed amongst the 24 strongest El

Niño events, in the period from 1895 to 2015, and lasted from April 1982 up to September 1983 (https://www.esrl.noaa.gov/psd/enso/climaterisks/years/top24enso.html). This 1983 El Niño effect was also detected in rainfall data over the São Paulo Metropolitan Area (Obregón et al., 2014), although the authors claim that such influence, at least on rainfall variability, is detectable but is multifaceted and depends on the life cycle of each ENSO event. Xavier et al. (1995), trying to identify a possible influence of ENSO on precipitation extremes in the month of May, classified both May 1983 and May 1987 as exceptional extremes of precipitation. Their conclusion was that strong El Niño events can affect the spatial organization of rainfall around São Paulo city. A more recent study performed by Coelho et al. (2017), using daily precipitation data from 1934 to 2013 from the same meteorological station analyzed in this research, concluded that El Niño conditions in July tend to increase precipitation in the following spring, also anticipating the onset of the rainy season. No study was found about the possible effect of ENSO on cloud cover over São Paulo. According to Rosas et al. (2019), middle and high level clouds presented high positive anomalous cloud amount in 1983.

After 1983, the trend behavior of ~~all~~ some variables changed, consistent with the findings of Reid et al. (2016), who observed a regime shift in land surface temperature in South America in 1984. Their results motivated ~~what motivated~~ us to separate the time series analysis in two periods, the first from 1961 to 1983 and the second from 1984 up to 2016. The results of the modified Mann-Kendall trend test for each period are presented in Table 2, considering both annual and seasonal variabilities. Bold values indicate trends that are statistically significant at the 95% confidence level. From the table, in the first period, SSR, SD and DTR presented a decreasing trend, while ~~SCF~~CCF a positive one, increasing at a rate of 2.9% per decade. Except for SSR, all

Formatado: Não Realce

trends were statistically significant, with daily SD decreasing at a rate of 0.37 hours per decade and the diurnal temperature range declining at a rate of 0.49°C per decade. Looking at the seasonal variability, southern hemisphere autumn (MAM) and winter (JJA) presented statistically significant decreasing trends for SSR, SD and DTR. Springtime (SON) presented statistically significant decreasing trends also for SD and DTR. For ~~SCF~~CCF, statistically significant positive trends were observed for JJA and SON only.

Table 2 - Modified Mann-Kendall trend test results for ~~P~~period~~eriod~~ 1, from 1961 to 1983, and ~~Pe~~period 2, from 1984 to 2016, considering each season and in an annual basis for the surface solar radiation (SSR), sunshine duration (SD), diurnal temperature range (DTR) and sky cover fraction (~~SCF~~CCF). The trend was estimated as the slope of the linear fit between the variable of interest and year.

SSR						
	Period 1: 1961-1983			**Period 2: 1984-2016**		
Time interval	**Trend[a]**	**Z**	**p**	**Trend[a]**	**Z**	**P**
Annual	-0.~~42~~40	-1.~~74~~64	0.~~081~~101	**-0.39~~41~~**	**-3.02~~18~~**	**0.003~~1~~**
DJF	-0.64~~6~~	-1.05~~11~~	0.291~~67~~	**-0.5~~4~~3**	**-2.56~~62~~**	**0.0110~~09~~**
MAM	**-0.76~~8~~**	**-2.48**	**0.013**	-0.~~26~~25	-1.66~~72~~	0.~~085~~097
JJA	-0.~~48~~47	-1.~~98~~93	0.054~~48~~	-0.17~~8~~	-1.~~97~~87	0.~~049~~061
SON	-0.~~25~~24	-0.~~96~~89	0.~~335~~373	**-0.~~58~~57**	**-2.~~46~~40**	**0.~~014~~016**
SD						
	Period 1: 1961-1983			**Period 2: 1984-2016**		
Time interval	**Trend[b]**	**Z**	**p**	**Trend[b]**	**Z**	**~~P~~p**
Annual	**-0.37**	**-3.41**	**0.001**	**0.11**	**2.13**	**0.033**
DJF	-0.41	-1.06	0.291	-0.01	-0.12	0.905

Formatado: Fonte: Não Negrito

MAM	**-0.53**	**-2.27**	**0.023**	0.22	1.61	0.107
JJA	**-0.54**	**-3.38**	**0.001**	**0.20**	**2.06**	**0.039**
SON	**-0.47**	**-2.31**	**0.021**	0.03	0.20	0.840
			DTR			
	Period 1: 1961-1983			**Period 2: 1984-2016**		
Time interval	**Trend[c]**	**Z**	**p**	**Trend[c]**	**Z**	**~~P~~p**
Annual	**-0.49**	**-3.33**	**0.001**	0.16	1.84	0.065
DJF	-0.32	-1.61	0.107	0.15	1.72	0.085
MAM	**-0.58**	**-2.54**	**0.011**	0.16	1.53	0.125
JJA	**-0.61**	**-2.91**	**0.004**	0.14	1.38	0.171
SON	**-0.58**	**-2.64**	**0.008**	0.02	0.17	0.865
			~~SCF~~CCF			
	Period 1: 1961-1983			**Period 2: 1984-2016**		
Time interval	**Trend[d]**	**Z**	**p**	**Trend[d]**	**Z**	**~~P~~p**
Annual	**2.9**	**2.48**	**0.013**	0.8	1.78	0.075
DJF	0.5	0.42	0.673	0.3	0.38	0.700
MAM	2.9	1.58	0.113	0.6	0.76	0.448
JJA	**3.5**	**2.54**	**0.011**	0.8	0.57	0.566
SON	**3.8**	**2.12**	**0.034**	1.5	1.22	0.221

Units of trend: a) kJ m^{-2} per decade; b) hours per decade; c) °C per decade; d) % per decade

In the first period, SSR and its proxies presented trends consistent with SFC features, i.e., as SFC increased over time, the others decreased. In the second period, from 1984 to 2016, this behavior combination changed. While SSR still presented, on an annual basis, a statistically significant decreasing trend, of -0.41 kJm^{-2} per decade, SD and DTR trends changed from negative to positive, being statistically significant only for SD, with a trend of 0.11 hours per decade. SFC CCF continued to present a positive trend, but not statistically significant. It is worth noting that, even though the trends are not statistically significant, the pattern between SSR and SFC CCF observed in the first period remained in the second, and in all seasons. According to Rosas et al. (2019), statistically significant trends, positive for low clouds (3.2% per decade) and negative for mid level clouds (-5.5% per decade), were observed in the last 30 years, from 1987 to 2016. Such analysis indicated that changes in cloud types also influenced the variability of SSR and proxies. However, other factors, rather than only cloud changes, were also responsible for the variability of SD and DTR, as analyzed in the next sections.

3.2 Long term variability of horizontal visibility and of the number of foggy days

Analysis of cloud free days

To verify how effectively the horizontal visibility acts as a proxy for aerosol optical depth, Fig. 3 shows the solar transmittance (SSR/TSR) and the normalized sunshine duration (n/N) for clear sky days, from July to October, as a function of daily mean visibility. The correlation coefficients are 0.57 and 0.52 for (SSR/TSR) and (n/N), respectively, as indicated in the figure, and for this reason, the visibility data will be analysed next as a proxy for aerosol optical depth. As mentioned in the methodology section, we excluded visibility data from early morning and late afternoon to minimize the influence of fog.

Formatado: Espaço Depois de: 6 pt, Espaçamento entre linhas: Duplo

Formatado: Fonte: Negrito

Formatado: Não Realce

Formatado: Espaço Depois de: 6 pt, Espaçamento entre linhas: Duplo

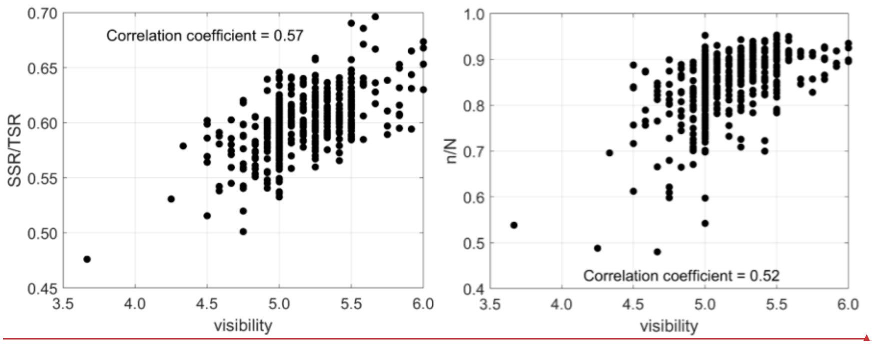

Figure 3 – Daily solar transmittance and the normalized sunshine duration as functions of the mean horizontal visibility recorded from 10:00 AM to 03:00 PM on clear sky days in the months of July to October.

Figure 4 presents the mean visibility from July to October and registered between 10:00 AM to 03:00 PM, and the number of foggy days in the same months, from 1961 to 2016, both for all sky conditions. July to October are the months with lower cloud cover fraction and with higher probability of long-range transport of biomass burning aerosol particles towards São Paulo, contributing to higher aerosol optical depth in the city (Castanho and Artaxo, 2001, Landulfo et al., 2003, Freitas et al., 2005, Castanho et al., 2008, Yamasoe et al., 2017). Since clear sky days are rare in São Paulo, here we discuss the long-term variability of visibility, trying to infer aerosol loading variations.

From the figure, we see that the highest visibility was observed during the first half of the 1960’s, with a gradual degradation till early 1970’s. From that, visibility increased again but never recovered to the values of the 1960’s. A significant reduction in visibility was observed in 1963. One hypothesis for the lower visibility in 1963 worth investigating was a sequence of vegetation fires reported in August and September in

Formatado: Não Realce

the state of Paraná affecting 128 municipalities (Paixão and Priori, 2015). Soares (1994) stated that about 10 % of Paraná state was affected by the fires, being responsible for the beginning of fire monitoring in Brazil due to its large proportion. Paraná is located to the south-southwest of São Paulo state. Cold front systems frequently advect air masses from the region towards São Paulo.

Considering local pollution sources, the reduction of the visibility data at the beginning of the series could be associated with the industrialization process in São Paulo, and with the vehicular fleet and changes in the fuel composition, at the end. According to Silva (2011), during 1956 to 1961, a national development plan was implemented in Brazil, to enhance the economic growth, what benefited particularly the city of São Paulo, attracting industries, mainly from the automobile sector. This contributed to increasing the city's population and to the concentration of industries, boosting the economy of São Paulo city. In the 1970's, the high rate of urbanization, with many traffic jams, caused air quality and environmental degradations (Silva, 2011). As one of the consequences, federal government promoted incentives to move industries to other Brazilian states, especially in the north and northeast regions of the country, but part remained in the Metropolitan Area of São Paulo. Still according to the author, this industrial decentralization process lasted till around 1991.

Andrade et al. (2017), discussing changes over time in air quality conditions at the Metropolitan Area of São Paulo, showed that SO_2 frequently exceeded the air quality standards in the 1970's and 1980's. According to the authors, the Brazilian government started a program to control its emission due to the complaints of the population. At the beginning, the program focused on stationary sources (industries) and, in the 1990's, the sulfur content in diesel fuel was also targeted. Nonetheless, during that decade, the Metropolitan Area of São Paulo still experienced severe air pollution problems with increasing concentration of aerosol particles, which might explain the reduction in visibility at the beginning of the decade (Fig. 4). Over time, SO_2 emission control and other measures helped decreasing the concentration of SO_2 and of particulate matter with diameter less than 10 µm (PM10) near the surface. However, according to Oyama (2015), also due to a political decision to stimulate the economy, the annual number of registrations of new gasoline fuelled vehicles increased exponentially, from about 3000 vehicles in 1988, peaking in 2000 with 150000 registrations, and decreasing slowly after that, to about 60000 in 2012. Despite the effort to reduce vehicular emission, the concentration of particulate matter with diameter less or equal 2.5 µm is not yet controlled. In the recent years, vehicular emission is the main local source of air pollution in the Metropolitan Area of São Paulo (Andrade et al., 2017).

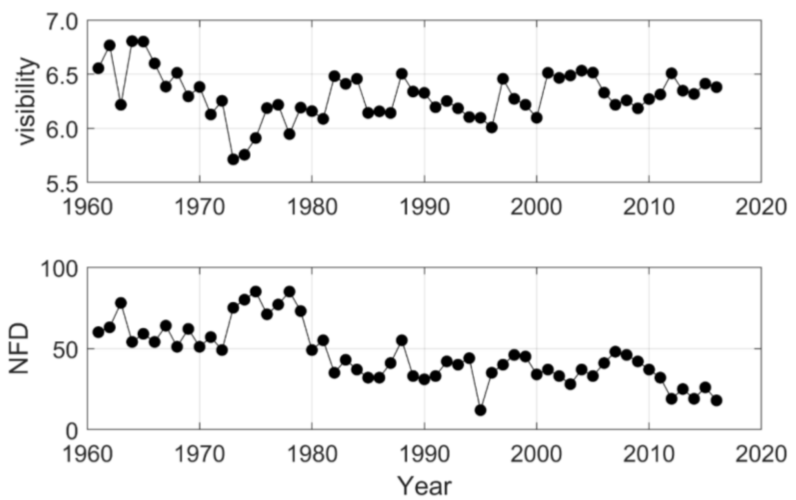

Formatado: Não Realce

Formatado: Não Realce

Figure 4 – Time series of the mean visibility recorded from 10:00 AM to 03:00 PM and the number of foggy days (NFD) per year in all sky conditions. Data are limited to the months of July to October.

Since both SSR and SD presented positive correlation with visibility, another factor might be responsible for the opposite trends observed in the second period for those variables. Changes in the number of foggy days are explored to verify if its variability can help to explain part of the variability observed in the SD trends, particularly after 1983, when CCF only could not explain it. As shown in Fig. 4, the number of days with fog, in the months of July to October each year, is decreasing in São Paulo. The highest numbers were observed during the 1970's with a sharp decrease in the end of the decade and the beginning of the next, followed by a long period of stable conditions up to 2011 when another decrease was observed. This could be the reason for the positive trend of SD under all sky scenarios in the second period (Fig. 2), when the CCF increase was not significant. A decrease in the annual number of foggy days was also observed in China (Li et al., 2012), which the authors attributed to the urban heat island effect. São Paulo, throughout the analysed period in this study, experienced a significant change in its spatial domain, which contributed to the intensification of the urban heat island effect. More on this effect will be discussed in the next section.From the good correlation between SSR and SFC, and based on previous results from Yamasoe et al. (2017), cloud cover seems to be the main driver of SSR attenuation in São Paulo. To evaluate the solely contribution of aerosol direct effect, we relied on a limited number of completely clear sky days since the current study was based on irradiation data, i.e., integrated from sunrise to sunset. However, in order to have a clue on its effect, mean atmospheric transmittance was estimated, during cloud free conditions, i.e., considering only days with SCF less than 0.1 and with, at least, 9 cloud free days per year. Most of those days were observed in winter and beginning of spring, when dry conditions prevail, aerosol loading related to local sources is higher and when biomass burning plumes from long range transport can be detected in São Paulo (Castanho and Artaxo, 2001, Landulfo et al., 2003, Freitas et al., 2005, Castanho et al., 2008, Yamasoe et al., 2017). For these reasons, we restricted this analysis using data from July to October only.

For the first period, the cloud free mean transmittance was 0.691 ± 0.029 and for the second period, a mean value of 0.700 ± 0.023 was estimated. Applying the Student t-test to compare the two means, we obtained $t = -0.87$ and $p = 0.40$, thus, the null hypothesis cannot be rejected at the 95% significance level, indicating that under cloudless sky the mean atmospheric transmittance over São Paulo was similar in both periods, suggesting that changes in the aerosol direct effect were unlikely to explain the distinct features observed in both periods. Nevertheless, from Figure 3, which illustrates the mean atmospheric transmittance (SSR/TSR) in cloud free conditions (i. e., SCF <= 0.1), in the first period, transmittance values were above 0.68, except in 1963, while in the second period transmittance below 0.68 were more frequent, which might suggest an increase in the atmospheric turbidity, particularly during the 1990's decade. However, it is worth mention a recovery to higher transmittance values after 2010. Similar features were also observed in n/N and horizontal visibility time series.

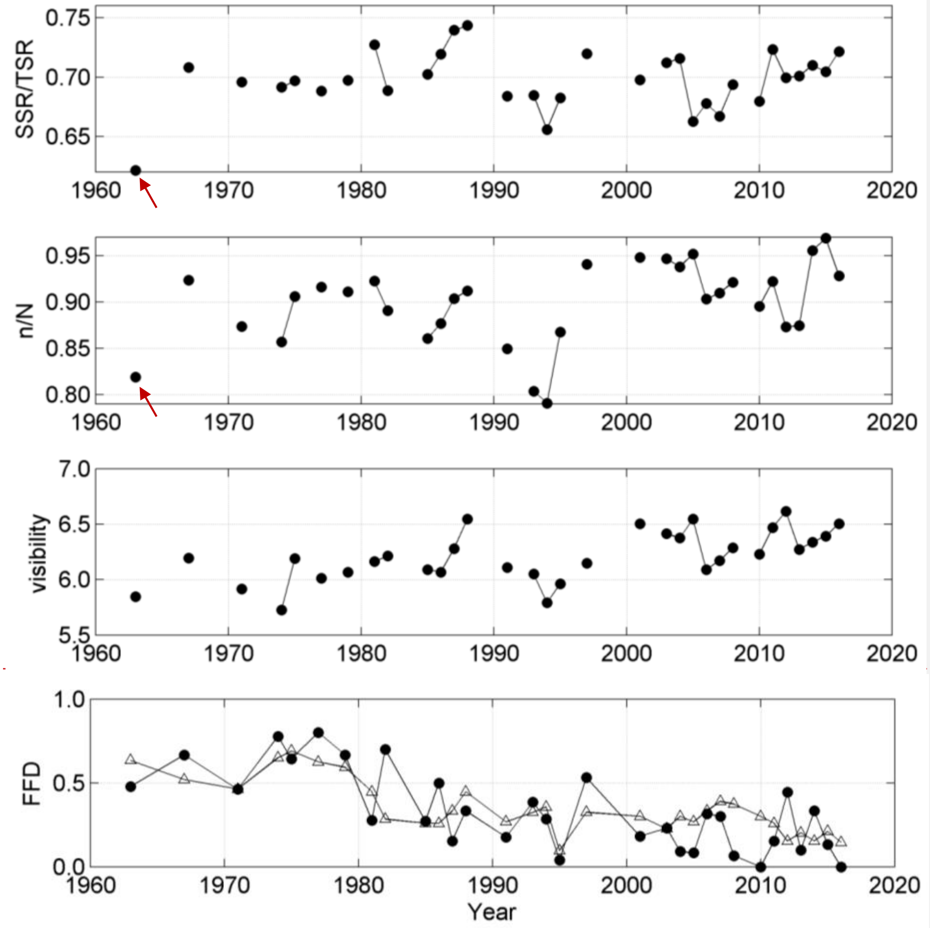

Figure 3 – Mean variability of cloud free (SCF <= 0.1) atmospheric transmittance (SSR/TSR), normalized sunshine duration (n/N), horizontal visibility and fraction of foggy days (FFD) from July to September in each year (open symbols) and on the cloud-free days only in the same period (full symbols). The red arrow indicates the year of volcano Agung eruption, in 1963, whose signal was detected in both SSR and SD data. Only years with more than 9 cloud-free days were considered.

Figure 3 also shows that 1963 presented the lowest mean transmittance in the series, and a decrease observed in the normalized sunshine duration series as well.

According to Robertson et al. (2001), following Sato et al. (1993), one possible explanation is the eruption of volcano Agung, whose plume affected southern latitudes, with stratospheric AOD above 0.1 even one year after the eruption. Pinatubo eruption in 1991 also contributed to a high load of stratospheric AOD around latitude 25° S, particularly one year after eruption, but no clear evidence was detected in our data.

Mean values of n/N varied from 0.841 ± 0.035, in the first period, to 0.852 ± 0.047, depicting a higher variability in the second one. Student t-test returned a t value of −0.71, with $p = 0.49$, again indicating no difference in both periods. In contrast, horizontal visibility mean value varied from 6.04 ± 0.17 to 6.27 ± 0.21 and the Student t-test returned $t = -3.21$ and $p = 0.005$, indicating that horizontal visibility in the second period was statistically higher than in the first period, at the 95% significance level. Both n/N and horizontal visibility for cloudless sky presented an increasing trend particularly after 2000 (Figure 3). A possible explanation for this behavior may be due to a reduction over time in the frequency of haze, fog and mist. Notice that transmittance is more sensitive to haze than n/N, since haze can last throughout the day, affecting continuously the transmittance, while, for the conditions observed in São Paulo, its efficiency to extinguish the direct solar beam is limited, therefore, yielding a lower impact on sunshine duration measurements. According to Stanhill et al. (2014), only when aerosol optical depth (AOD) exceeds 2 sunshine duration recorders can be sensitive to aerosol loadings and only early in the morning and late in the afternoon (Horseman et al., 2008). By contrast, fog exerts a significant effect on n/N, because its strongest impact occurs early in the morning when it is more frequent and when mostly of solar radiation is in the diffuse component. Moreover, the number of days with fog is decreasing in São Paulo, and particularly on the analyzed cloud free days, the fraction of foggy days (FFD) decreased throughout the years as illustrated in Figure 3, what can explain the increase of n/N in the recent years. This could also be the reason for the positive trend of SD under all sky scenarios in the second period (Figure 2), when the SFC increase was not significant. A decrease in the annual number of foggy days was also observed in China (Li et al., 2012), which the authors attributed to the urban heat island effect. As expected, horizontal visibility is also affected by the presence of fog, although from Figure 3, only fog cannot explain all the variability observed in cloudless sky conditions. During the late 1980's to early 1990's, transmittance, n/N and horizontal visibility presented a significant decay clearly not related to the decrease observed in the number of foggy days.

Concerning the urban heat island effect, the Metropolitan Area of São Paulo experienced a fast growth rate from 1980 to 2010. There were nearly 12 million inhabitants in 1980, and the population grew to about 21 million inhabitants in 2010 (Silva et al., 2017). According to the authors, the urban area increased from 874 km^2 to 2209 km^2, from 1962 to 2002. According to Kim and Baik (2002), the maximum UHI intensity is more pronounced in clear sky conditions, occurs more frequently at night than during the day, and decreases with increasing wind speed. However, Ferreira et al. (2012) reported that, in São Paulo, the urban heat island maximum effect was observed during day time, around 03:00 PM, and was associated with downward solar radiation heating the urban region in a more effective way than the rural surrounding areas.

3.3 Long term trends in daily maximum and minimum temperatures

Figure 4 presents the temporal variation of the annual mean of the daily maximum and minimum temperatures registered at the meteorological station, used to estimate DTR. As discussed in the last paragraphs, if the increasing trend in SD over the last years could be possibly attributed to the decreasing number of days per year with fog occurrence, we now hypothesize on the possible reasons for the increasing trend of

DTR in the second period. According to Dai et al. (1999), ~~it~~DTR should also respond to cloud cover and precipitation and thus to SSR variations. As discussed by the authors, clouds can reduce T_{max} and increase T_{min}, since they can reflect solar radiation back to space during daytime and emit thermal radiation down to the surface during the night, respectively. Such behaviors can be clearly seen in Figure 4, in the first period, and confirmed by the trend analysis presented in Table 3. During the dimming period, T_{max} presented a negative trend, while T_{min} an increasing one, statistically significant at 95% confidence level for the last variable. Similar behavior was observed by Wild et al. (2007) who argued that the decreasing trend of T_{max} is consistent with the negative trend of SSR, demonstrating that solar radiation deficit at the surface presented a clear effect on the surface temperature. Looking at the second period, from 1984 to 2016, both maximum and minimum temperatures presented increasing trend, statistically significant at the 95% confidence level, in the annual basis, of 0.25 °C per decade and 0.16 °C per decade, respectively. In this period, T_{min} trend was still in line with the increasing SFC trend, but as pointed out by Wild et al. (2007) could also be a response to the increasing levels of greenhouse gases as also pointed by de Abreu et al. (2019).

Table 3 - Modified Mann-Kendall trend test results for period 1, from 1961 to 1983, and period 2, from 1984 to 2016, considering each season and in an annual basis, for the daily maximum (T_{max}) and minimum (T_{min}) temperatures. The trend was estimated as the slope of the linear fit between the variable of interest and year.

			T_{max}			
	Period 1: 1961-1983			**Period 2: 1984-2016**		
Time interval	**Trend**	**Z**	**p**	**Trend**	**Z**	**P**
Annual	-0.11	-1.33	0.184	**0.25**	**2.15**	**0.031**
DJF	0.20	1.06	0.291	**0.33**	**2.07**	**0.038**

MAM	-0.15	-0.79	0.430	0.03	0.23	0.816
JJA	0.02	0.26	0.795	**0.33**	**2.68**	**0.007**
SON	-0.26	-0.63	0.526	0.36	1.72	0.085
			T_{min}			
	Period 1: 1961-1983			**Period 2: 1984-2016**		
Time interval	**Trend**	**Z**	**p**	**Trend**	**Z**	**P**
Annual	**0.56**	**2.54**	**0.011**	**0.16**	**2.15**	**0.031**
DJF	**0.53**	**2.96**	**0.003**	**0.13**	**2.68**	**0.007**
MAM	**0.52**	**2.71**	**0.007**	-0.07	-0.79	0.429
JJA	0.62	1.58	0.113	0.26	1.78	0.075
SON	-0.03	0.63	0.526	**0.26**	**2.43**	**0.015**

Units of trend: °C per decade

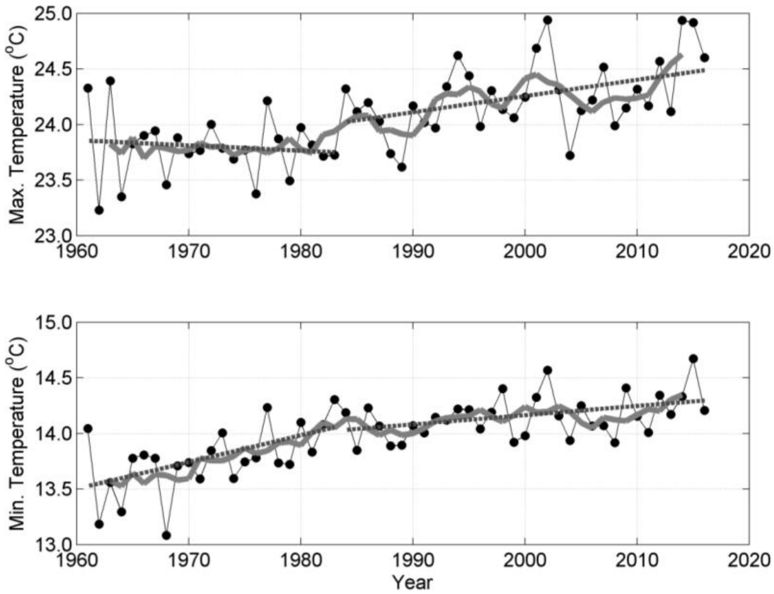

Figure 4 - Annual mean variability of daily maximum and minimum air temperatures at 1.5 meters. Gray curves represent 5 years moving averages and dotted lines are the result of trend analysis from 1961 to 1983 and from 1984 to 2016.

From the previous discussion, although completely cloud free days were extremely rare in São Paulo, the increase in T_{max} in the second period can be attributed to SSR changes associated with the aerosol direct effect only if the aerosol composition changed from a more scattering to a more absorbing one, with a similar attenuation effect on the solar radiation, as the atmospheric transmittance associated with aerosol only was similar in both periods. A recent study by Andrade et al. (2017), discussing changes over time in air quality conditions at the Metropolitan Area of São Paulo, showed that SO_2 frequently exceeded the air quality standards in the 1980's. According to the authors, the Brazilian government started a program to control its emission due to the complaints of the population. At the beginning, the program focused on stationary sources (industries) and, in the 1990's, the sulfur content in diesel fuel was also targeted. Thus, as a consequence of this program, SO_2 concentrations declined and other measures helped decreasing the concentration of particulate matter with diameter less than 10 µm (PM_{10}) near the surface. However, according to Oyama (2015), also due to a political decision to stimulate the economy, the annual number of registrations of new gasoline fueled vehicles increased exponentially, jumping from about 3000 vehicles in 1988, peaking in 2000 with 150000 registrations, decreasing slowly after that, to about 60000 in 2012.

Changes in aerosol chemical composition and consequently optical properties, from more scattering to more absorbing, without affecting the atmospheric transmissivity on cloud free days could possibly explain the effect on T_{max}. Sulfate, formed by gas to particle conversion of SO_2, is efficient as cloud condensation nuclei (Easter and Hobbs, 1974) and also presents high single scattering albedo (Takemura et al. 2002). Even with the renovation of the vehicular fleet in São Paulo, old heavy duty vehicles fueled with diesel still circulate in the MASP area, and according to Andrade et al. (2017) the diesel fleet constitute the main source of organic aerosols. In the case of diesel fueled vehicles, the number of new registered vehicles in the São Paulo city increased from about 5000 in 2000 to more than 25000 in 2010, the year with the highest number of registrations (Oyama, 2015). According to Feng et al. (2019), toluene secondary organic aerosol (SOA) presents low single scattering albedo in the ultraviolet-visible spectral range (0.78 ± 0.02) and toluene is one of the most abundant among the aromatic volatile hydrocarbons present in gasoline and other fuels (Brocco et al, 1997, Yamamoto et al., 2000). Particles with high absorption efficiency to solar radiation, such as black carbon, can cause heating of the atmosphere. According to Martins et al. (2009) aerosol particles measured during the wintertime of 1999 (August and September) presented high absorption efficiency in the ultraviolet spectrum, even higher than black carbon, which the authors attributed to the organic aerosol component. Previous results, from the AERONET (Aerosol Robotic Network) radiometer operating in the city, reported relative low single scattering albedo for aerosols from local sources, SSA at 550 nm around 0.85, (Castanho et al., 2008, Yamasoe et al., 2017).

In order to verify the possibility of a pattern change in aerosol properties, from a more scattering to a more absorbing one, without a significant change on aerosol attenuation capacity, at least during the second period, annual mean values of absorbing aerosol index and aerosol optical depth time series are presented in Figure 5. As mentioned previously, data only for the months of July, August, September and October were considered. For AAI, data are from 1979 to 2016 while for AOD, the MODIS in 2000 for Terra and 2002 for Aqua. Aerosol optical depth from MODIS onboard Terra and Aqua satellites Figure 5 presents the annual mean values time series. From the figure, annual mean AAI presented higher variability than mean AOD, particularly in the 1980 and 1990 decades, varying from 0.1 to 0.6 in the period. AOD, by contrast, varied from 0.13 to 0.28. Now, in order to verify possible trends, considering the second period only, i.e., from 1984 to 2016, the modified Mann-Kendall trend test was applied. A statistically significant positive trend of 0.07 AAI per decade, at 95% confidence level, was observed (Z = 2.81 and p = 0.005), consistent with the discussion from the previous paragraph. Since satellite retrieval of aerosol optical depth over land started only during the 2000's, no trend analysis was applied.

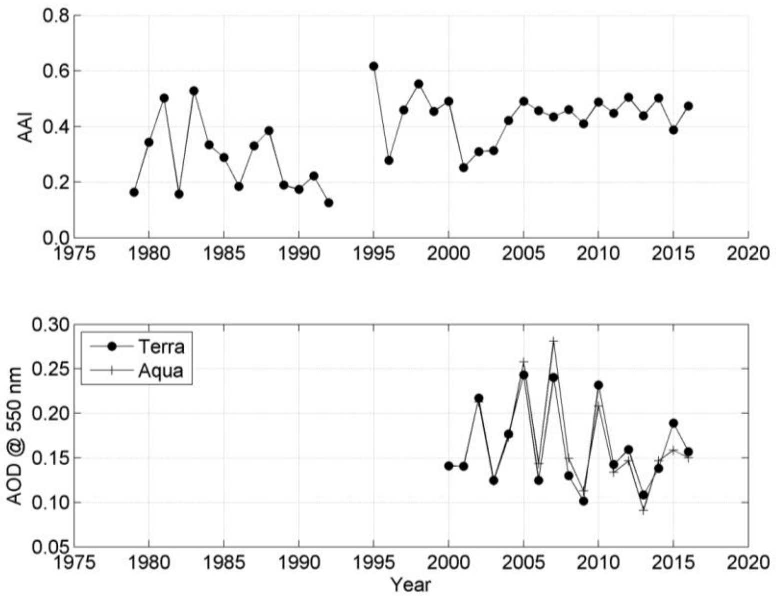

Figure 5 – Annual mean variability of absorbing aerosol index (AAI) (top) and aerosol optical depth (AOD) from MODIS onboard Terra and Aqua satellites (bottom).

The urban heat island effect could also be responsible to the observed increasing trend of T_{max}, particularly after 1980. The Metropolitan Area of São Paulo experienced a fast growth rate from 1980 to 2010. There were nearly 12 million inhabitants in 1980, and the population grew to about 21 million inhabitants in 2010 (Silva et al., 2017).

Formatado: Não Realce

According to the authors, the urban area increased from 874 km^2 to 2209 km^2, from 1962 to 2002. According to Kim and Baik (2002), the maximum UHI intensity is more pronounced in clear sky conditions, occurs more frequently at night than during the day, and decreases with increasing wind speed. However, Ferreira et al. (2012) reported that, in São Paulo, the urban heat island maximum effect was observed during daytime, around 03:00 PM, and was associated with downward solar radiation heating the urban region in a more effective way than the rural surrounding areas.

As discussed previously, due to the fast urbanization of the Metropolitan Area of São Paulo (Silva et al., 2017), the urban heat island effect could also be responsible to the observed increasing trend of T_{max}, particularly after 1980. Finally, as pointed by Wild et al. (2007), the increasing atmospheric concentration of greenhouse gases (GHG) can be another reason for the observed trend of T_{max}, which was masked by the dimming effect in the first period. Modeling studies can help verify the real causes and disentangle the contribution of each effect, which is, however, out of the scope of this work.

4 Conclusions

This analysis of 56 years of surface solar irradiation (SSR) and proxies (SD and DTR) data helped to show that from about 1960 to early 1980, named as first period, a dimming effect of surface solar radiation was observed in the city of São Paulo, consistent to other parts of the world. The positive trend of SCFCCF in the first period indicates that cloud variability could be one important driver of the dimming period. The dimming effect was also confirmed by SD and DTR trends in the mentioned period. However, the consistency between SSR, SD and DTR trends ended in 1983, when SCFCCF presented the highest value throughout the entire series and which coincided with a strong El Niño year. Thus, answering our first question, SSR presented a decreasing trend, throughout the 56 years of data, though not statistically significant at the 95% confidence level in the first period, while it decreased at a rate of -0.41 kJ m^{-2} per decade in the second one, from 1984 to 2016.

In the second period, the negative SSR trend was still consistent with the slight positive trend of ~~SCF~~CCF, while the opposite behavior of SD and DTR indicated that other factors besides the cloud cover variability might have affected their distinct patterns. In order to understand the possible causes of the SD trends, ~~a restrict analysis of~~ alternative parameters (fog frequency and horizontal visibility) focusing on ~~cloud free days, for~~ the dry months of July to October, were analyzed~~, in spite of the limited number of available days per year even allowing some flexibility (SCF <= 0.1)~~. The results indicated that the decreasing trend of the number of foggy days per year ~~is a potential candidate to~~ explains part of the increasing trend of SD~~ and horizontal visibility~~. ~~Although on cloud free days, no statistically significant difference was observed between SD in the first and the second period. Only horizontal visibility on cloud free days presented a statistically significant increase from the first to the second period. The analysis of cloud free days also showed that the effect of Agung volcano eruption was detected in both SSR and SD annual mean values. Due to Agung eruption, in 1963, the annual mean transmittance was the lowest in the series.~~

Moreover, on clear sky days, both SSR and SD presented correlation coefficients above 0.5 with visibility for the period when fog is unlikely to occur, indicating that this variable could be used as a proxy for aerosol loading variations. Changes in visibility during the 1960s and 1970s could be associated to the dynamics of the industrialization process of São Paulo Metropolitan Area and the consequent urbanization, with population growth, traffic jams and the degradation of the air quality. Long-range

Formatado: Não Realce

transport of biomass burning products towards São Paulo is also an important source of aerosol during the dry season. However, the long-term contribution of the different regions, as sources of pollutants to the atmosphere of the Metropolitan Area of São Paulo is unclear. The role of biomass burning, in the state of São Paulo and the neighbour states of Minas Gerais, Paraná and Mato Grosso, is yet to be clarified. Further research is needed to improve our historical perspective on the role of other regional air pollution sources on the SSR.

Formatado: Não Realce

In the case of DTR, since it was obtained from the difference between the daily maximum and minimum air temperatures close to the surface, the trends of the annual mean values of these temperatures were separately determined and analyzed. The T_{min} positive trends followed the ~~SCF~~CCF ones, with also possible influence of the increasing levels of greenhouse gases, noticing that the decay observed in ~~SCF~~CCF, in the beginning of the second period, is absent in the T_{min} time series. The increasing trend of ~~SCF~~CCF, in the first period, resulted in a decreasing trend in T_{max}, as more solar radiation reaching the surface was attenuated from year to year due to the presence of clouds. ~~One~~Some hypothes~~i~~es for the increasing trend of T_{max} during the second period ~~was the changing of aerosol optical properties in São Paulo, from a more scattering to a more absorbing one. Sulfate particles, which scatter solar radiation with high efficiency, had the emission of precursors to the atmosphere forced to decrease in the 1980's by governmental policies. However, other political decisions, to promote economic development, caused the increase of the gasoline fueled vehicles in São Paulo city in the beginning of the 1990's. Gasoline and other fuels are important sources of toluene, whose SOA presents very low single scattering albedo. The availability of an AERONET site in São Paulo, after 2000, made it possible to verify that the single scattering albedo of aerosol particles from local sources can be quite low. Data of~~

~~absorbing aerosol index retrieved from multiple satellites since 1979 and aerosol optical depth from MODIS onboard Terra and Aqua satellites were analyzed to verify the hypothesis of changing aerosol optical properties. The modified Mann-Kendall trend analysis for the AAI showed that this variable presented a positive trend statistically significant at 95% confidence level during the second period, although no trend analysis for AOD was performed because of the short time series available. Other hypotheses~~ are the urban heat island effect and the increasing concentrations of GHG. Of course, changes in the wind pattern and consequently in the advection of air masses with distinct properties can also affect the air temperature locally.

As the resultant trends of SD and DTR, compared with the SSR trend, diverged in the second period for São Paulo, in all sky conditions, caution might be taken when those variables are used as proxies to downward surface solar radiation in the context of dimming and brightening analyses. This study revealed that different factors may act on each variable, leading to a distinct behavior, as also mentioned by Manara et al. (2017).

For future studies, modeling efforts may be able to help evaluate each hypothesis raised in the present study, either those related to climate natural variability, such as El Niño, or to those arising from anthropogenic activities as the increase of greenhouse gas concentrations, land use changes, particularly through the imperviousness of soils, affecting the partitioning of latent and sensible heat fluxes. Also, higher temporal analysis and simultaneous monitoring of aerosol optical properties will help to better evaluate the aerosol effects on downward solar radiation in this region, including via the indirect effect.

Data availability

Access to IAG meteorological station database (sky cover fraction, sunshine duration, daily maximum and mimimum air temperatures, number of foggy days, visibility and irradiation data) for education or scientific use can be made under request at http://www.estacao.iag.usp.br/sol_dados.php. ~~The multi-sensor absorbing aerosol index was downloaded from http://www.temis.nl/airpollution/absaai/#MS_AAI, while AOD from MODIS on board Terra and Aqua satellites were obtained from https://giovanni.gsfc.nasa.gov/giovanni/.~~ All processed data used in the manuscript such as annual and seasonal mean values, as well as data from cloud free days can be found at https://www.iag.usp.br/lraa/index.php/data/cientec/weather-station-climatology/.

Author contribution

Conceptualization MAY and NMER; Methodology MAY; Data organization MAY and SNSMA; Formal analysis MAY; Writing original draft MAY and NMER; Writing – Review & Editing MAY, NMER, MW.

Competing interest

The authors declare that they have no conflict of interest.

Acknowledgements

The authors acknowledge Fundação de Amparo à Pesquisa do Estado de São Paulo (FAPESP), grant number 2018/16048-6 and Coordenação de Aperfeiçoamento de Pessoal de Nível Superior (CAPES) for financial support. Yamasoe acknowledges CNPq (Conselho Nacional de Desenvolvimento Cientifico e Tecnologico), process number 313005/2018-4. This study is part of the Núcleo de Apoio à Pesquisa em Mudanças Climáticas (INCLINE). The authors are grateful to the observers and staff of the Instituto de Astronomia, Geofísica e Ciências Atmosféricas meteorological station for making available the meteorological observations.

References

Andrade, M. F., Kumar, P., Freitas, E. D., Ynoue, R. Y., Martins, J., Martins, L. D., Nogueira, T., Perez-Martinez, P., Miranda, R. M., Albuquerque, T., Gonçalves, F. L. T., Oyama, B. and Zhang, Y. Air quality in the megacity of São Paulo: Evolution over the last 30 years and future perspectives. Atmospheric Environment 159, 66-82, 2017.

Bristow, K. L. and Campbell, G. S. On the relationship between incoming solar radiation and daily maximum and minimum temperature. Agricultural and Forest Meteorology 31, 159-166, 1984.

~~Brocco, D., Fratarcangelli, R., Lepore. L., Petricca, M. and Ventrone, I. Determination of aromatic hydrocarbons in urban air of Rome. Atmospheric Environment 31(4), 557-566, 1997.~~

Castanho, A. D. A. and Artaxo, P. Wintertime and summertime São Paulo aerosol source apportionment study. Atmospheric Environment 35, 4889-4902, 2001.

Castanho, A. D. de A., Martins, J. V. and Artaxo, P. MODIS aerosol optical depth retrievals with high spatial resolution over an urban area using the critical reflectance. J. Geophys. Res. 113, D02201, doi: 10.1029/2007JD008751, 2008.

Coelho, C. A. S., Firpo, M. A. F., Maia, A. H. N., and MacLachlan, C. Exploring the feasibility of empirical, dynamical and combined probabilistic rainy season onset forecasts for São Paulo, Brazil. Int. J. Climatol. 37 (Suppl. 1), 398-411, doi: 10.1002/joc.5010, 2017.

Dai, A., Trenberth, K. E. and Karl, T. R. Effects of clouds, soil moisture, precipitation, and water vapor on diurnal temperature range. Journal of Climate 12, 2451-2473, 1999.

de Abreu, R. C., Tett, S. F. B., Schurer, A. and Rocha, H. R. Attribution of detected temperature trends in Southeast Brazil. Geophysical Research Letters, 46, 8407–8414. https://doi.org/10.1029/2019GL083003, 2019.

Dutton, E. G., Stone, R. S., Nelson, D. W. and Mendonca, B. G. Recent interannual variations in solar radiation, cloudiness, and surface temperature at the South Pole. Journal of Climate 4, 848-858, 1991.

Easter, R. C. and Hobbs, P. V. The formation of sulfates and the enhancement of cloud condensation nuclei in clouds. Journal of the Atmospheric Sciences 31, 1586-1594, 1974.

Feng, Z., Huang, M., Cai, S., Xu, X., Yang, Z., Zhao, W., Hu, C., Gu, X. and Zhang, W. Characterization of single scattering albedo and chemical components of aged toluene secondary organic aerosol. Atmospheric Pollution Research 10, 1736-1744. doi: 10.1016/j.apr.2019.07.005, 2019.

Ferreira, M. J., Oliveira, A. P., Soares, J., Codato, G., Bárbaro, E. W. and Escobedo, J. F. Radiation balance at the surface in the city of São Paulo, Brazil: diurnal and seasonal variations. Theor. Appl. Climatol. 107-229-246. doi: 10.1007/s00704-011-0480-2, 2012.

Freitas, S. R., K. M. Longo, M. A. F. S. Dias, P. L. S. Dias, R. Chatfield, E. Prins, P. Artaxo, G. A. Grell, and F. S. Recuero. Monitoring the transport of biomass burning emissions in South America, Environ. Fluid Mech., 5, 135–167, 2005.

Graaf, M., Stammes, P., Torres, O., Koelemeijer, R. B. A. Absorbing Aerosol Index: Sensitivity analysis, application to GOME and comparison with TOMS. J. Geophys. Res. 110, D01201, doi: 10.1029/2004JD005178, 2005.

Hamed, K. H. and Rao, A. R. A modified Mann-Kendall trend test for autocorrelated data. Journal of Hydrology 204, 182-196, 1998.

Herman, J. R., Barthia, P. K., Torres, O., Hsu, C., Seftor, C. and Celarier, E. A. Global distributions of UV-absorbing aerosols from NIMBUS 7/TOMS data. J. Geophys. Res. 102(D14), 16911-16922, 1997.

Horseman, A., MacKenzie, A. R. and Timmis, R. Using bright sunshine at low-elevation angles to compile an historical record of the effect of aerosol on incoming solar radiation. Atmos. Environ. 42, 7600-7610, 2008.

Hsu, N. C., Tsay, S. C., King, M. D. and Herman, J. R. Aerosol properties over bright-reflecting source regions. IEEE Trans. Geosci. Remote Sens., 42, 557-569, 2004.

Kaufman, Y. J., Tanré, D., Remer, L., Vermote, E., Chu, A. Holben, B. N. Operational remote sensing of tropospheric aerosol over land from EOS Moderate Resolution Imaging Spectroradiometer. J. Geophys. Res. 102, 17051 – 17067, 1997.

Kazadzis, S., Founda, D., Psiloglou, B. E., Kambezidis, H., Mihalopoulos, N., Sanchez-Lorenzo, A., Meleti, C., Raptis, P. I., Pierros, F., and Nabat, P. Long-term series and trends in surface solar radiation in Athens, Greece, Atmos. Chem. Phys., 18, 2395–2411, https://doi.org/10.5194/acp-18-2395-2018, 2018.

Kim, Y.H. and Baik J. J. Maximum urban heat island intensity in Seoul. J. Appl. Meteorol, 41, 651–659, 2002.

Kren, A. C., Pilewskie, P. and Coddington, O. Where does Earth's atmosphere get its energy? J. Space Weather Space Clim. 7(A10) doi: 10.1051/swsc/2017007, 2017.

Kumari, B. P. and Goswami, B. N. Seminal role of clouds on solar dimming over India monsoon region. Geophys. Res. Letters 37 (L06703), 1-5, doi:10.1029/2009GL042133, 2010.

Landulfo, E., A. Papayannis, P. Artaxo, A. D. A. Castanho, A. Z. Freitas, R. F. Sousa, N. D. Vieira Jr., M. P. M. P. Jorge, O. R. Sánchez-Ccoyllo, and D. S. Moreira. Synergetic measurements of aerosols over São Paulo, Brazil using LIDAR, Sunphotometer and satellite data during the dry season, Atmos. Chem. Phys., 3, 1523–1539, 2003.

Li, Z., Yang, J., Shi, C. and Pu, M. Urbanization effects on fog in China: Field Research and Modeling. Pure Appl. Geophys. 169, 927-939, doi: 10.1007/s00024-011-0356-5, 2012.

Makowski, K., Wild, M. and Ohmura, A. Diurnal temperature range over Europe between 1950 and 2005. Atmos. Chem. Phys., 8, 6483–6498, 2008.

Manara, V., Brunetti, M., Celozzi, A., Maugeri, M., Sanchez-Lorenzo, A. and Wild, M. Detection of dimming/brightening in Italy from homogenized all-sky and clear-sky surface solar radiation records and underlying causes (1959-2013). Atmos. Chem. Phys. 16, 11145-11161, doi:10.5194/acp-16-11145-2016, 2016.

Manara, V., Brunetti, M., Maugeri, M., Sanchez-Lorenzo, A. and Wild, M. Sunshine duration and global radiation trends in Italy (1959–2013): To what extent do they agree? J. Geophys. Res. Atmos. 122, 4312–4331, doi:10.1002/2016JD026374, 2017.

Manara, V., Bassi, M., Brunetti, M. et al. 1990–2016 surface solar radiation variability and trend over the Piedmont region (northwest Italy). Theor. Appl. Climatol. 136, 849–862, doi: 10.1007/s00704-018-2521-6, 2019.

Martins, J. V., Artaxo, P., Kaufman, Y. J., Castanho, A. D. and Remer, L. A. Spectral absorption properties of aerosol particles from 350-2500 nm. Geophys. Res. Letters 36, L13810, doi: 10.1029/2009GL037435, 2009.

Obregón G. O., Marengo J. A. and Nobre C. A. Rainfall and climate variability: long-term trends in the Metropolitan Area of São Paulo in the 20th century. Clim Res 61:93-107. https://doi.org/10.3354/cr01241, 2014.

Ohvril, H., Teral, R., Neiman, L., Kannel, M., Uustare, M., Tee, M., Russak, V., Okulov, O., Jõeveer, A., Kallis, A., Ohvril, T., Terez, E. I., Terez, G. A., Gushchin, G. K., Abakumova, G. M., Gorbarenko, E. V., Tsvetkov, A. V. and Laulainen, N. Global dimming and brightening versus atmospheric column transparency, Europe, 1906-2007. J. Geophys. Res. 114(D00D12), 1-17, doi:10.1029/2008JD010644, 2009.

Oyama, B. S. Contribution of the vehicular emission to the organic aerosol composition in the city of São Paulo. (Doctoral Thesis). Universidade de São Paulo, São Paulo, Brazil. Available at https://www.iag.usp.br/pos/sites/default/files/t_beatriz_s_oyama_corrigida.pdf - last access on October 25, 2019, 2015.

Paixão, L. A. and Priori, A. A. Social and environmental transformations of the rural landscape after an environmental disaster (Paraná, Brazil, 1963). Estudos Históricos 28(56), 323-342, http://dx.doi.org/10.1590/S0103-21862015000200006, 2015.

Paltridge, G. W. and Platt, C. M. R. Radiative processes in meteorology and climatology. Elsevier Science, Amsterdam, Oxford, New York, 1976.

Plana-Fattori, A. and Ceballos, J. C. Algumas análises do comportamento de um actinógrafo bimetálico Fuess modelo 58d. Revista Brasileira de Meteorologia 3 (2), 247-256, 1988.

Raichijk, C. Observed trends in sunshine duration over South America. International Journal of Climatology 32, 669-680. ~~Doi~~doi: 10.1002/joc.2296, 2012.

Reid, P. C., Hari, R. E., Beaugrand, G., Livingstone, D. M., Marty, C., Straile, D., Barichivich, J., Goberville, E., Adrian, R., Aono, Yasuyuki, Brown, R., Foster, J. Groisman, P., Hélaouët, P., Hsu, H.-H., Kirby, R., Knight, J., Kraberg, A., Li, J., Lo, T.-T., Myneni, R. B., North, R. P., Pounds, J. A., Sparks, T., Stübi, R., Tian, Y., Wiltshire, K. H., Xiao, D. and Zhu, Z. Global impacts of the 1980s regime shift. Global Change Biology 22, 682-703. doi: 10.1111/gcb.13106, 2016.

~~Remer, L. A., Kaufman, Y. J., Tanre, D., Mattoo, S., Chu, D. A., Martins, J. V., Li, R. R. , Ichoku, C., Levy, R. C., Kleidman, R. G., Eck, T. F., Vermote, E. and B. N. Holben, B. N. The MODIS aerosol algorithm, products and validation. J. Atmos. Sci., 62, 947-973, 2005.~~

~~Robertson, A., Overpeck, J., Rind, D., Mosley-Thompson, E., Zielinski, G., Lean, J., Koch, D., Penner, J., Tegen, I. and Healy, R. Hypothesized climate forcing time series for the last 500 years. J. Geophys. Res. 106(D14), 14783-214803, 2001.~~

Rosas, J., Yamasoe, M. A., Sena E. T. and Rosário N. E. Cloud climatology from visual observations at São Paulo, Brazil. Int. J. Climatol., 1–13. https://doi.org/10.1002/joc.6203, 2019.

~~Sato, M., Hansen, J. E., McCormick, M. P. and Pollack, J. B. Stratospheric aerosol optical depths, 1850-1990. J. Geophys. Res. 98(D12), 22987-22994, 1993.~~

Sen, P. K. Estimates of the regression coefficient based on Kendall's Tau. Journal of the American Statistical Association 63(324), 1379-1389, 1968.

Shi, G., Hayasaka, T., Ohmura, A., Chen, Z.-H., Wang, B., Zhao, J.-Q., Che, H.-Z. and Xu, Li. Data quality assessment and the long-term trend of ground solar radiation in China. Journal of Applied Meteorology and Climatology 47, 1006-1016, 2008.

Silva, F. B., Longo, K. M., and Andrade, F. M. Spatial and temporal variability patterns of the urban heat island in São Paulo. Environments 4, 27, doi: 10.3390/environments4020027, 2017.

Silva, P. F. J. Notas sobre a industrialização no estado de São Paulo, Brasil. Finisterra, XLVI 91, 87-98, 2011.

Stanhill, G. and Cohen, S. Global dimming: a review of the evidence for a widespread and significant reduction in global radiation with discussion of its probable causes and possible agricultural consequences. Agricultural and Forest Meteorology 107, 255-278, 2001.

Stanhill, G., Achiman, O., Rosa, R. and Cohen, S. The cause of solar dimming and brightening at the Earth's surface during the last half century: Evidence from measurements of sunshine duration. J. Geophys. Res. Atmos. 119, 10902-10911. doi:10.1002/2013JD021308, 2014~~)~~.

~~Takemura, T., Nakajima, T., Dubovik, O., Holben, B. N. and Kinne, S. Single-scattering albedo and radiative forcing of various aerosol species with a global three-dimensional model. Journal of Climate 15(4), 333-352, 2002.~~

~~Tilstra, L. G., Graaf, M., Tuinder, O. N. E., van der A, R. J., and Stammes, P. Monitoring aerosol presence over a 15-year period using the Absorbing Aerosol Index measured by GOME-1, SCIAMACHY, and GOME-2, Proceedings of the ESA Living Planet Symposium 2013, ESA Special Publication SP-722, 2014.~~

~~Torres, O., Barthia, P. K., Herman. J. R., Ahmad, Z. and Gleason, J. Derivationof aerosol properties from satellite measurements of backscattered ultraviolet radiation: Theoretical basis. J. Geophys. Res. 103(D14), 17099-17110, 1998.~~

Xavier, T. M. B. S., Silva Dias, M. A. F. and Xavier, A. F. S. Impact of ENSO episodes on the autumn rainfall patterns near São Paulo, Brazil. Int. J. Climatol. 15. 571-584, 1995.

Wild, M., Gilgen, H., Roesch, A., Ohmura, A., Long, C. N., Dutton, E. G., Forgan, B., Kallis, A., Russak, V., and Tsvetkov, A. From dimming to brightening: decadal changes in solar radiation at Earth's surface. Science 308, 847-850, 2005.

Wild, M., Ohmura, A., and Makowski, K. Impact of global dimming and brightening on global warming. Geophys. Res. Lett. 34, L04702, doi: 10.1029/2006GL028031, 2007.

Wild, M. Global dimming and brightening: A review. J. Geophys. Res. 114(D00D16), doi: 10.1029/2008JD011470, 2009.

Wild, M. Enlightening global dimming and brightening. BAMS 93, 27-37, doi:10.1175/BAMS-D-11-00074.1, 2012.

Wild, M., Folini, D., Schär, C., Loeb, N., Dutton, E. G. and König-Langlo, G. The global energy balance from a surface perspective. Clim. Dyn. 40, 3107-3134, doi: 10.1007/s00382-012-1569-8, 2013.

Wild, M. Towards global estimates of the surface energy budget. Curr. Clim. Change Rep. 3, 87-97. doi: 10.1007/s40641-017-0058-x, 2017.

~~Yamamoto, N. Okayasu, H., Murayama, S., Mori, S., Hunahashi, K. and Suzuki. Measurement of volatile organic compounds in the urban atmosphere of Yokohama, Japan, by an automated gas chromatographic system. Atmospheric Environment 34, 4441-4446, 2000.~~

Yamasoe, M. A., N. M. E. do Rosário, and K. M. Barros. Downward solar global irradiance at the surface in São Paulo city—The climatological effects of aerosol and clouds, J. Geophys. Res. Atmos., 122, 391–404, doi:10.1002/2016JD025585, 2017.

Yang, S., Wang, X. L. and Wild, M. Causes of Dimming and Brightening in China Inferred from Homogenized Daily Clear-Sky and All-Sky in situ Surface Solar Radiation Records (1958-2016). Journal of Climate 32, 5901-5913, doi: 10.1175/JCLI-D-18-0666.1, 2019.

Zerefos, C.S., Eleftheratos, K., Meleti, C., Kazadzis, S., Romanou, A., Ichoku, C., Tselioudis, G. and Bais, A. Solar dimming and brightening over Thessaloniki, Greece, and Beijing, China. Tellus B, 61: 657-665. doi:10.1111/j.1600-0889.2009.00425.x, 2009.

Zhang, S., W., J., Fan. W., Yang, Q. and Zhao, D. Review of aerosol optical depth retrieval using visibility data. Earth-Science Reviews 200, 102986, https://doi.org/10.1016/j.earscirev.2019.102986, 2020.